Image Reconstructions of Microtubules Decorated with Monomeric and Dimeric Kinesins: Comparison with X-Ray Structure and Implications for Motility

A. Hoenger,* S. Sack,‡ M. Thormählen,‡ A. Marx,‡ J. Müller,‡ H. Gross,* and E. Mandelkow‡

*Institute of Cell Biology, Swiss Federal Institute of Technology, ETH-Hönggerberg, CH-8093 Zürich, Switzerland; and
‡Max-Planck-Unit for Structural Molecular Biology, D-22603 Hamburg, Germany

Abstract. We have decorated microtubules with monomeric and dimeric kinesin constructs, studied their structure by cryoelectron microscopy and three-dimensional image reconstruction, and compared the results with the x-ray crystal structure of monomeric and dimeric kinesin. A monomeric kinesin construct (rK354, containing only a short neck helix insufficient for coiled-coil formation) decorates microtubules with a stoichiometry of one kinesin head per tubulin subunit (α–β-heterodimer). The orientation of the kinesin head (an anterograde motor) on the microtubule surface is similar to that of ncd (a retrograde motor). A longer kinesin construct (rK379) forms a dimer because of the longer neck helix forming a coiled-coil. Unexpectedly, this construct also decorates the microtubule with a stoichiometry of one head per tubulin subunit, and the orientation is similar to that of the monomeric construct. This means that the interaction with microtubules causes the two heads of a kinesin dimer to separate sufficiently so that they can bind to two different tubulin subunits. This result is in contrast to recent models and can be explained by assuming that the tubulin–kinesin interaction is antagonistic to the coiled-coil interaction within a kinesin dimer.

Intracellular transport, mitosis, flagellar beating, and many other motile phenomena in cells are based on the interaction between microtubules and their motor proteins such as kinesins or dynein. The diverse family of kinesin-related motor proteins can be subdivided into two main classes, depending on whether they move their cargoes (e.g., vesicles, organelles) towards the plus end or the minus end of microtubules (anterograde or retrograde transport in axons). Their best known representatives are kinesin itself (a plus end–directed motor) and ncd (a minus end–directed motor). These proteins consist of several domains, the "head" or motor domain (containing the microtubule and ATP binding sites), a "stalk," which is largely α-helical and causes two kinesin chains to dimerize via a coiled-coil interaction, and a "tail" connecting the stalk to the cargo (for reviews see Goldstein, 1993; Brady, 1995; Cole and Scholey, 1995).

The core motor domain contains ~330 residues. Its x-ray structure has been solved recently for human kinesin and *Drosophila* ncd; despite their opposite directionality the two structures are remarkably similar (Kull et al., 1996; Sablin et al., 1996). There is a central β sheet of eight strands sandwiched between three α helices on either side. The residues interacting with microtubules are confined to the "rear" surface (containing loops L8, L12, and helices α4–α6; see Kull et al., 1996; Woehlke et al., 1997), whereas the "front" surface contains the nucleotide-binding loops (for review see Vale and Fletterick, 1997). A recent x-ray structure of rat kinesin in the monomeric and dimeric state has revealed additional features (Kozielski et al., 1997*a,b*; Sack et al., 1997). Notably, the NH_2-terminal entry and COOH-terminal exit of the polypeptide chain into the core motor domain have a β strand structure, forming an additional antiparallel β sheet (β0, β9) or integrated into the central sheet (β10). Conserved residues that play a role in the directionality of the motors (Case et al., 1997) are located around β9 for kinesin and near β0 for ncd. The neck helix α7 (Ala339–Trp370) extends from the lower tip of the structure, roughly within the plane of the core sheet. Judging from model peptides, the first half of the neck helix has a low coiled-coil potential, presumably because of its unusually high charge and nonstandard heptad residues, but the second half is similar to a leucine zipper and causes tight association (Morii et al., 1997; Tripet et al., 1997; Thormählen et al., 1998*b*). Accordingly, the con-

Address all correspondence to Dr. E. Mandelkow, Max-Planck-Unit for Structural molecular Biology, Notkestrasse 85, D-22603 Hamburg, Germany. Tel.: 49-40-8998-2810. Fax: 49-40-8971-6822. E-mail: mandelkow@mpasmb.desy.de

A. Hoenger's present address is European Molecular Biology Laboratory, Meyerhofstrasse 1, D-69012 Heidelberg, Germany.

struct rK354 is monomeric in solution and in the crystal, whereas rK379 is dimeric (Kozielski et al., 1997*a*).

The interaction between kinesin and tubulin has been probed by various biochemical and biophysical methods. Binding and cross-linking studies suggest that the motor domain interacts mainly with β-tubulin (Song and Mandelkow, 1993; Kikkawa et al., 1995), although some interactions also occur with α-tubulin (Walker, 1995; Tucker and Goldstein, 1997). Reports on the stoichiometry of binding have been controversial, claiming either one motor head bound per tubulin heterodimer (Harrison et al., 1993; Song and Mandelkow, 1993), or two (Huang et al., 1994; Lockhart et al., 1995). The latter value was interpreted within the framework of an "alternating catalysis" model of ATP exchange (Hackney, 1994; Gilbert et al., 1995; Ma and Taylor, 1997), whereby one head was firmly bound (and unable to exchange ATP) whereas the other was loosely tethered (and able to exchange ADP for ATP). A recent reinvestigation of the stoichiometry with scanning transmission electron microscopy, x-ray scattering, and other methods has confirmed the value of one head per tubulin heterodimer (Thormählen et al., 1998*a*; Marx et al., 1998), consistent with the results reported below. Measurements of the movement of kinesin-coated beads along microtubules by laser trap microscopy has revealed a step size of 8 nm, equivalent to the axial spacing of tubulin heterodimers (Svoboda et al., 1993; Coppin et al., 1996; Hua et al., 1997; Inoue et al., 1997; Schnitzer and Block, 1997). Depending on the model of motion ("walking," "tightrope," and others; Cross, 1995; Howard, 1996) the observed step size for the kinesin dimer implies that a single head must be able to translocate up to 16 nm. This is remarkably large considering the head's small dimensions of $\sim 6 \times 3.5 \times 3$ nm.

Several image reconstructions of microtubules decorated with kinesin and ncd have been presented recently. There is good agreement on the shape and position of monomeric constructs (Hirose et al., 1995, 1996; Hoenger et al., 1995; Kikkawa et al., 1995; Arnal et al., 1996; Hoenger and Milligan, 1997; Sosa et al., 1997*b*; for comparison see Figs. 2 and 3 below). Roughly speaking, if we view a microtubule in standard orientation (with the fast-growing "plus" end up) the tubulin subunits show an anticlockwise slew, the bound motor heads are attached mostly to β-tubulin (with some overlap to α-tubulin) with the long axis roughly vertical, and with a clockwise displacement relative to the tubulin subunits (similar to Fig. 4 below). This shape could be fitted well with the x-ray structure of monomeric ncd, showing the sequences implicated in microtubule interactions (loops L2, L8, L11, L12, helices α4, and α6 on the rear surface) touching the microtubule surface (Sosa et al., 1997*a*).There was however a curious discrepancy when dimeric constructs of kinesin or ncd were used (Arnal et al., 1996; Hirose et al., 1996). Microtubules decorated with dimeric ncd showed two complete heads per tubulin heterodimer, one bound directly to the microtubule surface (very similar to the monomeric constructs), the second one attached to the first head, with an anticlockwise slew, and pointing towards the microtubule minus end. This arrangement was consistent with the stoichiometry of two motor heads per tubulin subunit (Huang et al., 1994; Crevel et al., 1996). In the case of dimeric kinesin, however, the additional mass accounted for only ~20% of a head, and it pointed towards the microtubule plus end. This mass increase was interpreted to mean that a second head was present but only partially visible because of disorder. The differences between kinesin and ncd in the orientation of the second head were thought to reflect the different mechanisms of motility (plus versus minus end directed).

An alternative explanation for kinesin, presented here, is that there is only one bound head per tubulin heterodimer so that an additional mass observed with a dimeric construct would be simply explainable by the longer neck, rather than an additional but disordered head. We find that the electron density decorating the microtubule surface agrees well with the x-ray structure of the kinesin monomer, but not with the x-ray structure of the kinesin dimer. This implies that the two heads of dimeric kinesin separate substantially upon binding to the microtubule lattice such that each head attaches to a different tubulin subunit. The orientation of the kinesin monomer is similar to that of the ncd monomer described by Sosa et al. (1997*a*), and the α-helical neck projects from the upper end of the molecule in an anticlockwise direction. Thus the crest of a protofilament appears to be embraced between loop L11 and the neck helix α7. The observed separation of the heads would be sufficient to allow each head to make large steps along the microtubule, in spite of the small head size. The conserved "gearbox" residues that are important for the directionality of motors (Case et al., 1997; Henningsen and Schliwa, 1997) are located in the upper part of the bound kinesin, near the head–neck junction.

Materials and Methods

Assembly of Microtubules

Tubulin was prepared by phosphocellulose chromatography preceded by a MAP-depleting step as described (Mandelkow et al., 1985). Microtubules were polymerized in reassembly buffer (0.1 M Pipes, pH 6.9, 1 mM $MgCl_2$, 0.5 mM EGTA, 1 mM DTT, 20 μM taxol) and 1 mM GTP from a solution containing 6–15 mg/ml of PC-tubulin on incubation at 37°C for 20 min.

Expression of Kinesin

Plasmids coding for rat kinesin constructs were cloned and expressed as described in Kozielski et al.(1997*a*). Briefly, to obtain pErK379 the BamHI–SauI fragment of the rat kinesin gene (provided by S. Brady, University of Texas, Dallas, TX) was inserted into a pET-3a vector modified to contain the same sites with a stop codon. Plasmid pErK354 was cloned by PCR using plasmid pErK379 as a template. The plasmids were expressed in *Escherichia coli* BL21 (DE3) cells. Recombinant rK354 and rK379 could be obtained in soluble form from the bacterial extracts. *E. coli* cells were grown in Luria-Bertani (LB) medium and expression of kinesin was induced with 0.4 mM isopropylthio-β-D-galactoside (IPTG) at a cell density corresponding to A_{600} = 0.6–0.8. Cells were harvested after 16 h of induction at 25°C, resuspended in lysis buffer (50 mM Pipes, pH 6.9, 60 mM NaCl, 1 mM $MgCl_2$, 0.5 mM EGTA, 2 mM DTT, 1 mM PMSF), and then lysed with a French press. Purification was done by ion exchange chromatography on phosphocellulose and MonoQ followed by gel filtration on a G-200 Hiload 16/60 column (Pharmacia Biotechnology Inc., Piscataway, NJ).

Kinesin–Microtubule Binding Assays

Stoichiometries and dissociation constants were determined essentially as described (Thormählen et al., 1998*a*). Briefly, taxol-stabilized microtubules at a concentration of 4 μM were incubated with kinesin (≤20 μM kinesin heads) in the presence of 2 mM 5′-adenylylimidodiphosphate

(AMP-PNP)[1]. Microtubules with bound kinesin were pelleted in an ultracentrifuge (TL100; Beckman Instruments, Inc., Fullerton, CA) at 67,000 *g* and 22°C for 10 min. The pellets and supernatants were analyzed by SDS-PAGE. Coomassie blue–stained dried gels were digitized and evaluated by using the software TINA (Raytest, Straubenhardt, FRG).

Decoration of Microtubules with Kinesin

Microtubules were polymerized for 20 min at 37°C in 80 mM Pipes, pH 6.8, 2 mM $MgCl_2$, at a concentration of 2.5 mg/ml and in the presence of 5% (vol/vol) DMSO, 2 mM GTP, and 20 μM taxol. Polymerized tubulin was washed twice by centrifugation in a centrifuge (Eppendorf Inc., Madison, WI), and resuspended in GTP-free buffer. Decoration of polymerized microtubules with rK354 was performed in solution at a final tubulin concentration of 1 mg/ml (~10 μM) and a final kinesin concentration of 1.5 mg/ml (~30–40 μM, depending on construct) and in the presence of 2 mM AMP-PNP. This stoichiometry was found previously (Hoenger and Milligan, 1997) to yield complete decoration. Samples were incubated for 2 min and subsequently adsorbed to holey carbon grids for 1 min, and then quick-frozen in liquid propane by using a plunger essentially following the standard procedures described initially by Dubochet et al. (1985). Decoration of microtubules with rK379 was performed directly on the grid to avoid bundling of tubules, either in the presence of 2 mM AMP-PNP, or in the absence of nucleotides. To this end, microtubules at a concentration of 1 mg/ml were adsorbed on holey carbon grids for 1 min, washed briefly, and then incubated with a rK379 solution at 3 mg/ml (to obtain the same stoichiometry as for rK354 = approximately two kinesin double heads per tubulin dimer) for 2 min and quick-frozen as described above.

Cryoelectron Microscopy

Cryoelectron microscopy was performed on a CM12 microscope (Philips Electron Optics, Mahwah, NJ) equipped with an ultra-high vacuum chamber (MIDILAB; Gross et al., 1990) and a modified GATAN cryoholder that allowed the grid to be transferred from the MIDILAB to the holder without passing through air. The MIDILAB allowed storage of four frozen grids simultaneously at liquid N_2 temperature in ultra-high vacuum, which were readily available for a fast transfer into the microscope. In addition, we used the carbon evaporating capabilities of this chamber to coat the frozen grids with a thin layer of carbon (30 Hz = ~3 nm) before observation to reduce charging effects on the grids. Micrographs were recorded at a magnification of 35,000× on SCIENTIA electron microscopy film (AGFA, Leverkusen, Germany) (developed for 4 min in KODAK D19) at an electron dose of $<5\ e^-/Å^2$. Images were taken at a defocus range between −1 and −1.5 μm. On the CM12 twin lens microscope this defocus range places the first zero node of the contrast transfer function between 1/27 and 1/20 Å.

Image Processing and Three-Dimensional Reconstruction

Because of the lattice properties of microtubules (Mandelkow et al., 1986; Wade et al., 1990; Sosa and Milligan, 1996; Sosa et al., 1997*b*) we were searching for microtubules that exhibit a Moirè pattern (Mandelkow and Mandelkow, 1985; Wade et al., 1990) corresponding to 15-protofilament/2-start helical microtubules (Sosa et al., 1997*b*). They accounted for ~5% of the total number of microtubules present in a solution polymerized in the presence of 5% DMSO (see above). 15-protofilament/2-start helical microtubules also exhibit a characteristic diffraction patterns as shown in Fig. 2. Micrographs were digitized using a Leaf scanner (Leaf Systems, Westborough, MA) operated at a pixel size of 20 μm on the negative, which amounts to 0.57 nm on the sample. Suitable 15-protofilament/2-start microtubules were helically reconstructed by using the software package PHOELIX (Whittaker et al., 1995*a*). Some of them were long enough to be prescreened for multiple seams by back projection (Wade et al., 1995; Sosa and Milligan, 1996), but such cases were not observed. One data set represents a near or far side of an intact microtubule; the microtubules had an average length of ~1.2 μm corresponding to ~150 tubulin dimers per protofilament. A total of 19 data sets were used for the reconstruction of microtubules decorated with rK379 in the presence of AMP-PNP, 10 data sets went into the reconstructions of microtubules decorated with rK379 in the absence of nucleotide, 8 data sets were processed for microtubules decorated with rK354 (+AMP-PNP), and 14 data sets were used to reconstruct the undecorated microtubule control map. Table I summarizes the specific data for each reconstruction. All data sets were truncated to a maximum resolution of 20 Å. Three-dimensional maps were visualized by using the software packages SUPRIM (Schroeter and Bretaudiere, 1996), and SYNUVIEW (Hessler et al., 1996). The three-dimensional maps of decorated microtubules were supplemented with the x-ray structure of rK379 by using "O" (Jones et al., 1991). All calculations were performed on an INDIGO workstation (Impact-10000; Silicon Graphics, Inc., Mountain View, CA). The polarity of the maps presented here was determined according to Hoenger and Milligan (1996). All maps are shown in a standard orientation (plus end up).

Difference Mapping and t Tests

Difference maps were calculated to investigate the possibility of a residual signal from the second head (missing or dislocated) of rK379-decorated microtubules. All maps were brought to the same phase origin and subtracted from each other. We performed *t* tests to assess the statistical significance of the differences obtained. To this end we calculated variance maps from single and double head–decorated maps that contained 8 (rK354) and 19 (rK379) individual phase-aligned maps. For comparison, the maps from rK354-decorated microtubules were also tested against the undecorated microtubules (14 individual maps). This provided a calibration of the signal since the difference is due to a well-defined motor head domain. All calculations were carried out with the "varimap" and "*t* test" routines provided by PHOELIX.

Results

Electron Microscopy Three-dimensional Reconstructions Reveal Only a Single Head of Kinesin per Tubulin Heterodimer, Both for Monomeric and "Dimeric" Kinesin

Kinesin constructs containing the motor domain but without or with only a short neck domain are monomeric in solution, while increasing lengths of the neck lead to dimerization because of their coiled-coil interactions (Huang et al., 1994; Correia et al., 1995; Jiang et al., 1997). Thus, since monomeric kinesin head domains bind to microtubules with a stoichiometry of one head per tubulin subunit (= α–β-heterodimer, mostly at β-tubulin; Song and Mandelkow, 1993), one would expect dimeric constructs to bind to two tubulin heterodimers, i.e., with the same stoichiometry of one kinesin head per tubulin heterodimer. This is illustrated in Fig. 1 for the case of the dimeric construct rK379; results on other monomeric or dimeric constructs obtained with different methods are described elsewhere (Thormählen et al., 1998*a*). In this regard, kinesin

Table I. Summary of Data Sets Used for the Three-dimensional Reconstructions

Reconstruction	MT + rK379 (AMP-PNP)	MT + rK379 (no nucl.)	MT + rK354 (AMP-PNP)	Undecorated microtubules
No. of datasets	19	10	8	14
No. of asymmetrical units	21,000	11,000	10,500	15,500
Average phase residual (degrees)				
correct	21.0 ± 5.0	28.3 ± 6.1	17.9 ± 2.8	19.7 ± 3.5
opposite orientation	55.3 ± 6.1	52.4 ± 7.0	54.7 ± 3.9	33.3 ± 4.5

Common orientations were determined on the basis of phase residual comparisons that clearly discriminate between the "up" and "down" orientation. Each data set accounts for one near or far side of the helix. The average phase residual is shown for the alignments incorrect and opposite (upside down) orientation. The large difference reflects the polarity of the three-dimensional reconstructions.

1. *Abbreviation used in this paper*: AMP-PNP, 5′-adenylylimidodiphosphate.

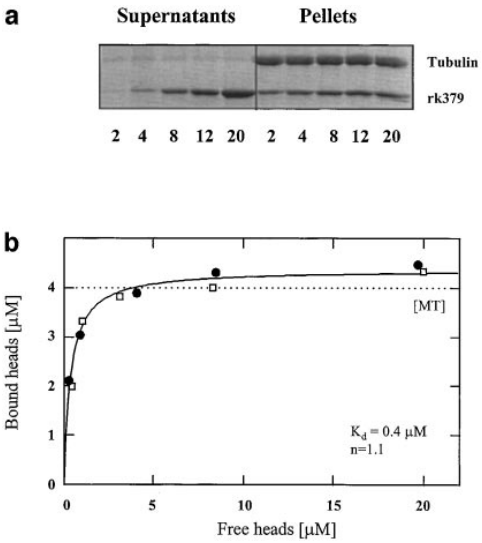

Figure 1. Example of a binding experiment of kinesin construct rK379. This construct forms a compact and tightly bound dimer in solution and crystallizes in dimeric form (Kozielski et al., 1997*b*). (*a*) SDS gel showing supernatants and pellets of a binding experiment in the presence of 2 mM AMP-PNP. Concentrations of kinesin heads range from 2 to 20 μM as indicated, the concentration of tubulin heterodimers is 4 μM. (*b*) Graph showing bound versus free kinesin heads. The binding curve yields a dissociation constant of 0.4 μM and a stoichiometry of 1.1 μM kinesin heads per μM tubulin dimer, equivalent to one kinesin dimer per two tubulin heterodimers.

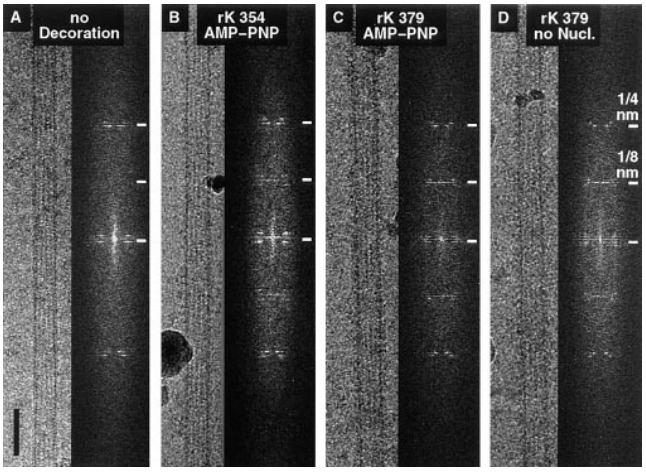

Figure 2. Cryoelectron micrographs of 15-protofilament microtubules. *A*, without kinesin decoration; *B*, decorated with rK354 in the presence of AMP-PNP; *C*, decorated with rK379 in the presence of AMP-PNP; and *D*, decorated with rK379 in the absence of nucleotide. The computed diffraction patterns are shown beside the images; note the pronounced layer line at 1/8 nm in *B*, *C*, and *D* resulting from the presence of kinesin (for details of the layer line analysis see Sosa et al., 1996). Bar, 50 nm.

differs from the retrograde motor ncd whose dimeric constructs bind with a stoichiometry of two heads per tubulin subunit (Crevel et al., 1996). Note however that the results on dimeric kinesin are in contrast to those derived from two recent cryoelectron microscopy studies (Arnal et al., 1996; Hirose et al., 1996), which were interpreted in terms of two bound heads per tubulin subunit, similar to ncd (see Discussion).

Cryoelectron micrographs of microtubules decorated with kinesin constructs rK354 (monomeric in solution) and rK379 (dimeric) are shown in Fig. 2. The microtubules chosen for processing had 15 protofilaments because this allows helical image reconstructions without the complication of a seam asymmetry that is typical for the more common 13-protofilament microtubules (Sosa and Milligan, 1996; Sosa et al., 1997*b*). The diffraction patterns of the decorated particles reveal an additional set of strong layer lines ~1/8 nm, corresponding to the axial spacing of the decorating kinesin molecules (Fig. 2, *B–D*). This is equivalent to the spacing of tubulin heterodimers, consistent with biochemical and other data showing that kinesin interacts predominantly with β-tubulin (Song and Mandelkow, 1993; Kikkawa et al., 1995; Thormählen et al., 1998*a*). The reconstructed densities derived from the decorated microtubules (Fig. 3; averages of ~10,000–20,000 asymmetric units = tubulin dimers) display two features. There is a hollow cylinder (mean radius ~12.1 nm) consisting of 15 density peaks that represent the protofilaments seen in an end-on projection (from plus to minus end), slewing in an anticlockwise direction (see undecorated microtubule, Fig. 3 *A*; the left half is overlaid with the density contour lines). After decoration with kinesin a further density peak appears attached to each protofilament, centered at a radius of ~16.6 nm and displaced in a clockwise direction (Fig. 3, *B–D*). This density is very similar for both the monomeric construct rK354 (Figs. 3 *B* and 4 *A*) and the "dimeric" construct rK379, and its shape is nearly independent of the nucleotide status of kinesin (*AMP-PNP* in Figs. 3, *B* and *C*, and 4 *B*, or no nucleotide, Figs. 3 *D* and 4 *C*). Overall, these maps are similar to those obtained with human kinesin hK349 (Hoenger and Milligan, 1997; Sosa et al., 1997*b*). By contrast, microtubules decorated with a dimeric construct of the retrograde motor ncd showed two additional densities attached to each protofilament, one centered at an ~16.6-nm radius (as before), the second at ~19.9 nm, displaced in an anticlockwise direction (Fig. 3 *E*; see Hoenger and Milligan, 1997; Sosa et al., 1997*a*).

A statistical analysis using the *t* test procedure was applied to obtain a comparison of motor related mass densities between microtubules decorated with rK354 and rK379 (Fig. 3, *F–H*). Both maps were reconstructed from motor head domains in the presence of AMP-PNP. As a control, we compared the map of rK354-decorated microtubules with the nondecorated microtubules to obtain a direct measure of the difference signal resulting from a well-defined motor head domain (Fig. 3 *H*). The comparison between maps from microtubules decorated with rK354 or rK379 revealed no significant mass attributable to a second head in the vicinity of the first head attached to tubulin (Fig. 3, *F* and *G*). We found slight differences in mass at the end of every attached head in the plus-end direction (Fig. 3, *F* and *G*, *small arrow*). This would be consistent with the 25–amino acid mass increase of rK379 over rK354 within the neck helix. A second faint difference peak is located on the outer surface of the attached motor (Fig. 3, *F* and *G*, *long arrow*). However, these differences are small,

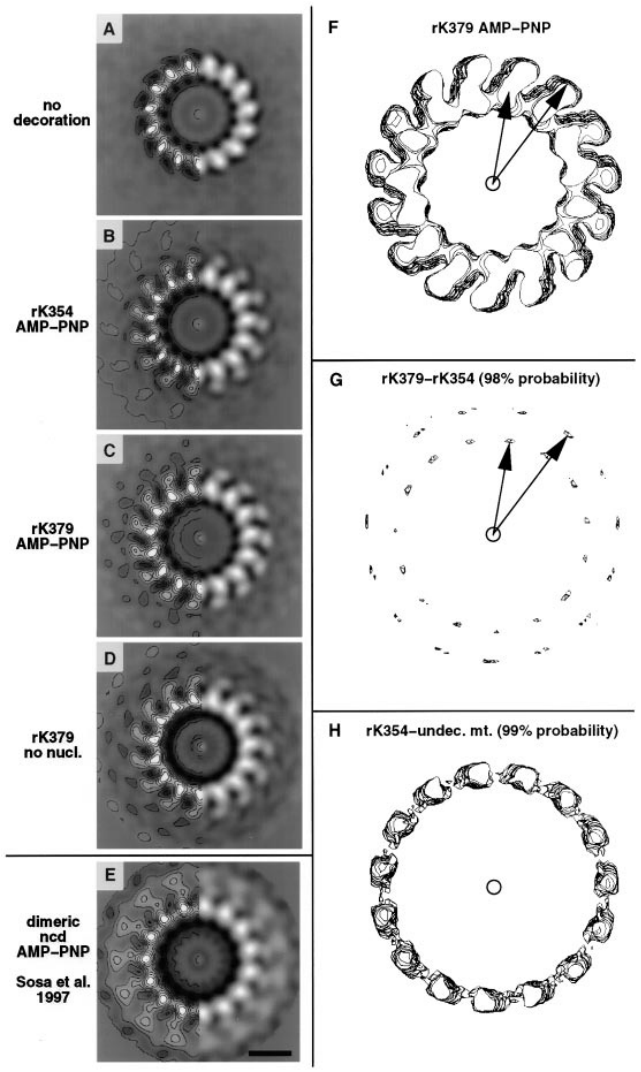

Figure 3. Left, axial projections of reconstructed tubulin–kinesin complexes, seen in the direction from the plus to the minus end. All reconstructions were done with 15-protofilament microtubules. (*A*) Undecorated microtubule; note the anticlockwise slew of the protofilaments. (*B*) Microtubule decorated with the monomeric kinesin construct rK354 in the presence of AMP-PNP. The additional mass outside the microtubule cylinder is equivalent to one bound kinesin head per tubulin heterodimer. The bound head shows a clockwise direction relative to the microtubule protofilaments. (*C*) Microtubule (15 protofilaments) decorated with the dimeric kinesin construct rK379 in the presence of AMP-PNP. Here too, the additional mass is equivalent only to one head per tubulin dimer. There is no indication of other additional mass in the vicinity of the bound head. (*D*) Similar reconstruction as in *C* but in the absence of nucleotide. As in *C* there is only one head per tubulin heterodimer. (*E*) A microtubule decorated with the dimeric ncd construct Dm-ncd450 is shown for comparison (data from Sosa et al., 1997*a*). Contrary to kinesin, this reconstruction clearly shows two heads of ncd bound per tubulin heterodimer, one bound firmly to the microtubule surface, the second tethered to the surface of the bound head and showing an anticlockwise slew. *Right*, significance of differences in mass between the double-headed rK379 construct and the single-headed rK354 construct, as assessed by *t* tests. All the graphs shown here are the axial projections of three dimensional volumes. 19 individual maps of rK379 reconstructions and 8 individual maps of rK354 reconstructions were compared with each other (both from decorated microtubules in the presence of AMP-PNP). The control between rK379 and no decoration was performed with another 14 undecorated microtubule reconstructions. (*F*) Full map drawn as an axially projected contour plot (note anticlockwise slew of tubulin at the inner densities and the clockwise displacement of kinesin at the outer densities). (*G*) Contours that enclose areas with a 98% probability of mass differences between their constructions made with rK379 and rK354. The enclosed volumes are minute and there are no more detectable contours at 99%. As a control, we made the same statistical difference analysis between the rK354 reconstruction and the undecorated tubulin. The plot at the bottom of the column shows the resulting contours enclosing areas with 99% probability of difference, revealing essentially the added density of kinesin. Arrows in *F* and *G* point to corresponding areas on the maps.

they disappear at the 98% confidence level and thus could not account for a second attached head.

The fact that both rK354 and rK379 show only one attached head per tubulin heterodimer is consistent with the stoichiometry (Fig. 1). Nevertheless, it was still unexpected considering that the arrangement of heads in the crystal structure is very different. This implies a major conformational change between the solute and bound states of dimeric kinesin (Kozielski et al., 1997*a*; Marx et al., 1998; and see below). The volumes associated with the motor mass are clearly equivalent to the volume of one head only (Fig. 3, *B–D*). As shown later, the motor-related volume can be filled completely with the x-ray–derived map of one motor domain (Fig. 5). There may be subtle differences in the attached kinesin heads between the no-nucleotide and AMP-PNP states, but at the resolution shown here they are minute and shall therefore not be discussed in further detail. What matters is that the no-nucleotide state is the same as with AMP-PNP present: there is only one head attached to a tubulin subunit, and the second one is not visible.

The results described above become even more obvious on the three-dimensional surface-rendered maps shown in Fig. 4 where the volumes are adjusted approximately to the molecular weights of the components. The volume of the tubulin component is shown in blue. The monomeric construct rK354 (Fig. 4 *A*, *green*), the dimeric construct rK379 with AMP-PNP (Fig. 4 *C*, *yellow*) or without nucleotide (Fig. 4 *C*, *red*) have similar densities, equivalent to one motor head per tubulin heterodimer, and there is no evidence for additional motor mass in the case of microtubules decorated with "dimeric" rK379 (Fig. 4, *B* and *C*). By contrast, a large additional volume equivalent to a second tethered head is found on microtubules decorated with dimeric ncd (Fig. 4 *D*, *white* and *red*; Sosa et al., 1997*a*).

Orientation of the Bound Kinesin Head on Microtubules: Rear Surface Towards Tubulin, Neck Helix on Upper End and Tangential to Microtubule

The next step in the analysis was to interpret the low resolution kinesin density attached to microtubules in terms of the high resolution x-ray model of kinesin. The structures of the motor domains of human kinesin and *Drosophila* ncd have been solved and shown to be closely related (Kull et al., 1996; Sablin et al., 1996). They consist of a core

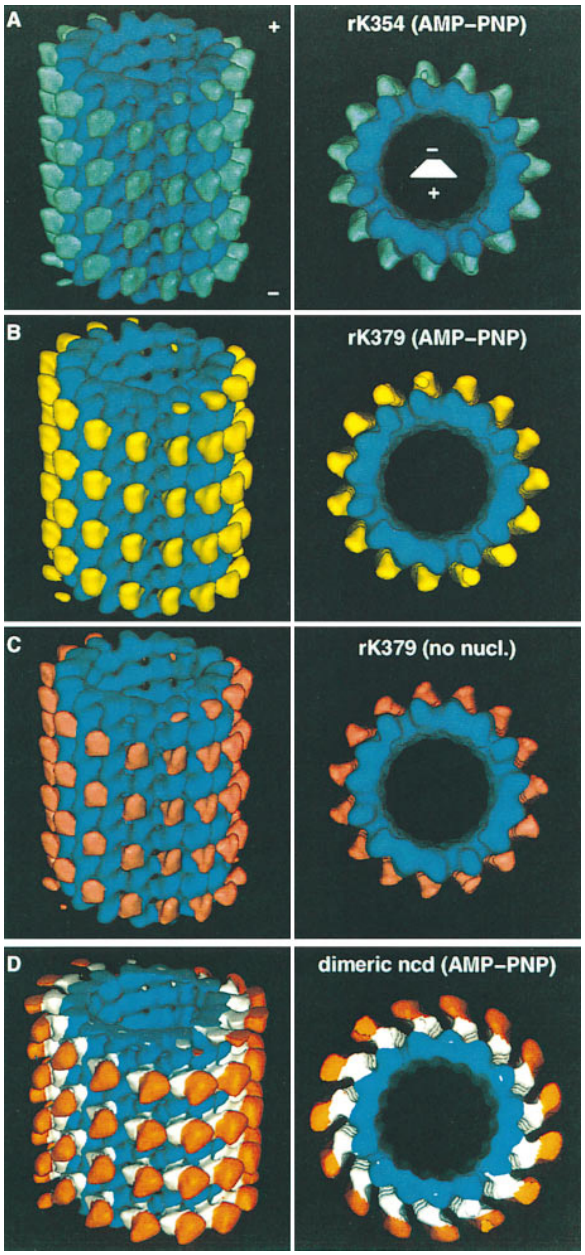

Figure 4. Surface rendered image reconstructions of decorated microtubules in front view (*left*, microtubule plus end up) and top view (*right*, seen from plus to minus end). Tubulin subunits are blue, motor proteins are in different colors. *A*, microtubule decorated with the kinesin construct rK354 (with AMP-PNP); *B*, with construct rK379 (with AMP-PNP); *C*, with construct rK379 (without nucleotide); and *D*, with the ncd construct Dm-ncd450 (data from Sosa et al., 1997*a*). Whereas in the case of ncd a second motor head tethered to the first is clearly visible (see *D*), it is absent in the case of kinesin (*B* and *C*). The firmly bound head has a similar position in both cases.

β sheet sandwiched between three α helices on either side; the front face contains the nucleotide binding site, the rear face contains the presumptive microtubule-binding region. The two heads of dimeric ncd have been fitted into the image reconstruction (Sosa et al., 1997*a*). More recently, the x-ray structures of the monomeric construct rK354 from rat brain kinesin and the dimeric construct rK379 have been solved (Kozielski et al., 1997*a*; Sack et al., 1997). The core motor domains were found to be similar to those of human kinesin and ncd, and in addition the structures revealed the positions of the NH_2- and COOH-terminal regions, including the COOH-terminal neck helix, α7. The coiled-coil interaction of this helix leads to the dimerization, as in the construct rK379. It would therefore be natural to assume that the crystal structures of kinesin monomers and dimers would fit into the reconstructed densities observed for the same constructs bound to microtubules (Fig. 5).

To orient the kinesin molecule on the microtubule surface, we first note that the reconstructed kinesin density has an elongated shape, ~6 × 3.5 × 3 nm, and the long axis runs parallel to the protofilaments (best seen in Fig. 5, *E* and *F*). The x-ray model of kinesin and ncd have similar dimensions (the "flower bouquet structure;" see Fig. 1 in Kull et al., 1996) so the long axes of the image reconstruction and x-ray models must roughly coincide. The next criterium comes from sequence conservation and mutagenesis experiments. All conserved loops implied in microtubule binding are on the rear face of the structure (e.g., L12, L8, helices α4 and α5; Kull et al., 1996), and an exchange of critical residues on this surface affects both microtubule binding and motility (Woehlke et al., 1997). Thus the rear surface of the kinesin head must be placed at the interface between the motor and tubulin. This leaves two main choices, the flower bouquet of the motor domain could be either "up" or "down." The orientation up (as in Fig. 1 of Kull et al., 1996) would mean that the nucleotide-binding site is near the top end (towards the plus end of microtubules), the neck helix near the bottom; down is the opposite. The down orientation is strongly preferred by several observations. First, the overall match between the x-ray structure of the motor domain and the reconstructed density is better (note the pointed tip on the upper right of the reconstructed density in Fig. 5 *E*, which marks the beginning of the neck helix). Second, the down orientation places loop L11 (not visible in the x-ray structure because of disorder) near its position in the analogous motor ncd (where L11 is ordered and visible), i.e., at the upper end of the density, pointing clockwise. The up orientation is sterically forbidden because loop L11 would penetrate into the microtubule surface. Third, Arnal et al. (1996) and Hirose et al. (1996) presented difference maps of dimeric kinesin constructs with monomeric ones, which both revealed the location of additional mass towards the plus end of the microtubule, pointing anticlockwise. In our down orientation this would coincide with the transition to the neck helix (Fig. 5, *E* and *F*, *upper right*)

These considerations yield the orientation of the motor domain shown in Fig. 5 (e.g., Fig. 5, *A*, *C*, and *E*, *yellow*; or *B*, *D*, and *F*, *blue*). In front view (Fig. 5 *E*), the kinesin head (*yellow*) appears suspended on the neck helix protruding at the upper end to the right. The orientation can be visualized by the "left hand down" rule: because the β strands run roughly vertical in this orientation, the view can be compared with that of a left hand pointing down and viewed from inside (thumb at upper right representing the neck helix). The microtubule-binding loops (on the back of the hand) would lean against the protofilament in

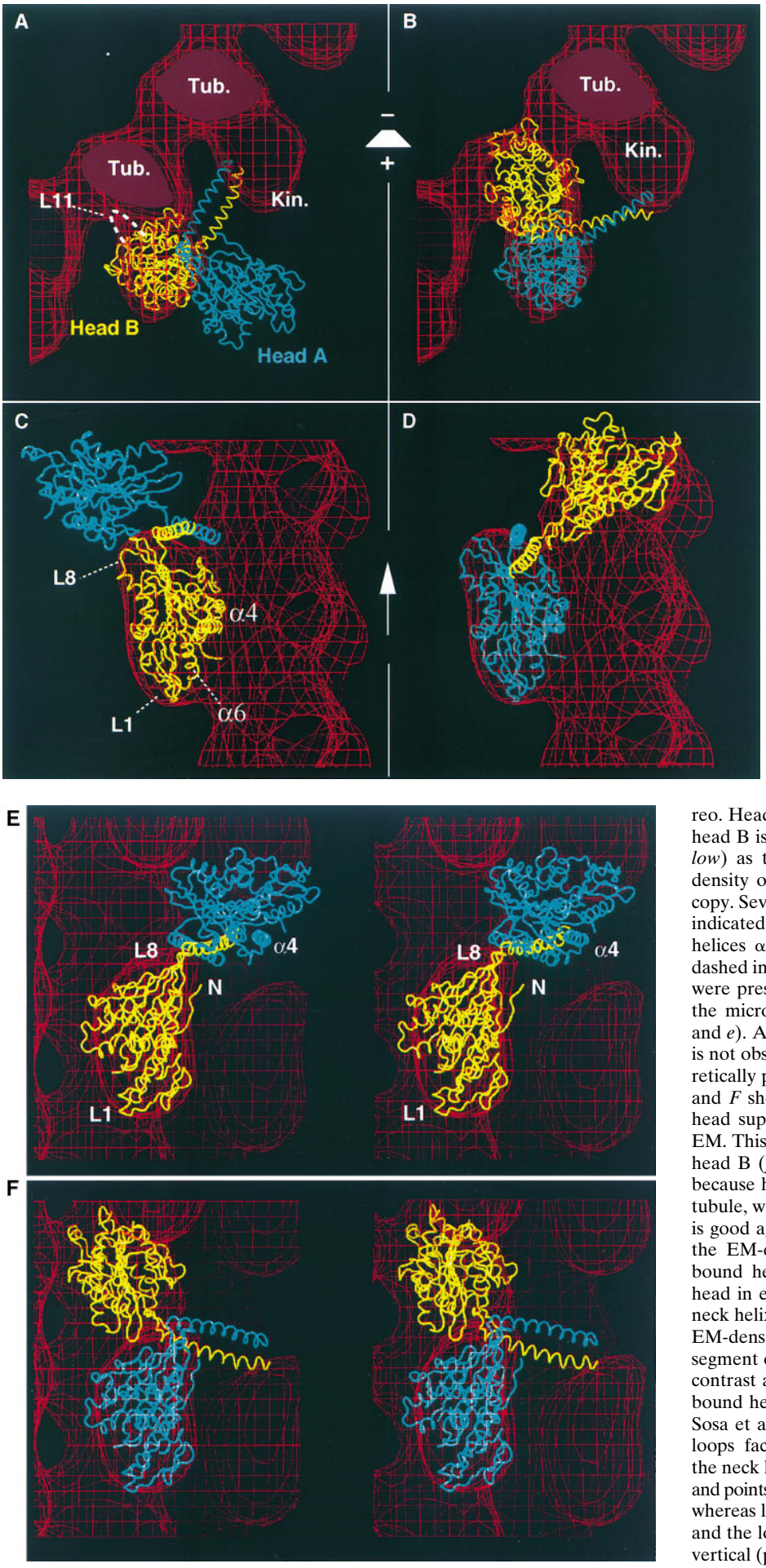

Figure 5. Superposition of the EM-derived, three-dimensional reconstruction (*red chicken-wire surface*) of microtubules decorated with the construct rK379 with the x-ray structure of the rK379 dimer (carbon backbone representation). *A* and *B*, top views (viewed from plus to minus end); *C* and *D*, lateral views of decorated protofilaments (cutaway of left edge of microtubule); *E* and *F*, front views in stereo. Head A of the x-ray dimer structure is blue, head B is yellow. *A*, *C*, and *E* show head B (*yellow*) as the tightly bound head, occupying the density of kinesin observed by electron microscopy. Several elements of the motor structure are indicated to facilitate orientation (loops L1, L8, helices α4). The likely position of loop L11 is dashed in *A* in analogy with ncd. If head A (*blue*) were present it would occupy free space outside the microtubule envelope above head B (see *c* and *e*). Although a second attached kinesin head is not observed, this arrangement would be theoretically possible without steric constraints. *B*, *D*, and *F* show head A (*blue*) as the firmly bound head superimposed on the density observed by EM. This cannot be matched with the position of head B (*yellow*) observed in the x-ray structure because head B would penetrate into the microtubule, which is physically impossible. Thus there is good agreement between the x-ray model and the EM-derived envelope for the microtubule-bound head, but no agreement for the second head in either orientation. The beginning of the neck helix matches well with a little "nose" in the EM-density (*e* and *f*, *upper right*), but the outer segment of the neck is not visible (due to lack of contrast and/or disorder). The orientation of the bound head is similar to that of the ncd head in Sosa et al. (1997*a*), i.e., the microtubule binding loops face towards the tubulin protofilaments; the neck helix α7 is at the upper end of the motor and points tangentially in an anticlockwise direction, whereas loop L11 points clockwise (*white dashes*), and the long axis of the motor domain is roughly vertical (parallel to the tubulin protofilaments).

the background (Fig. 5 *E*, *red wire frame*). Fig. 5 *C* shows a side view of the kinesin structure (*yellow*) extending from the left edge of a microtubule; the neck projects roughly towards the observer helix (stretched out "thumb"). In the top view (Fig. 5 *A*, *yellow*), the front of a microtubule is seen from above (plus end), the neck helix of the bound kinesin (*yellow*) projects to the right (anticlockwise), and loop L11 to the left (clockwise). This view illustrates how the microtubule-binding surface of kinesin is embraced between loop L11 and the neck helix on both sides, and that the neck helix points tangentially to the microtubule surface, which has consequences for models of motility (see Discussion). In this picture, the "gearbox" residues that are involved in the directionality (Case et al., 1997) and lie around strand β9 of kinesin, would correspond to the upper end of the second finger, near the force-transmitting neck helix.

Whereas the core of the head fits well into the reconstructed density, most of the neck helix appears to lie outside the volume enclosed by the map (except the initial segment). This can be explained by at least two factors: (*a*) α helices (single or coiled-coils) have very low contrast in cryoelectron microscopy at ~2-nm resolution; and (*b*) the necks could moreover be disordered or partly attached and merged with the density of tubulin so that they would not be visible as distinct entities.

Gedankenspiel: How Could Dimeric Kinesin Be Oriented on the Microtubule Surface?

In the above discussion we have concentrated on one kinesin head bound to the microtubule surface for every tubulin heterodimer. The orientation is appropriate for the monomeric construct rK354. However, rK379 is dimeric in solution and in the crystals, owing to its coiled-coil interaction (Kozielski et al., 1997*a*; Marx et al., 1998), and one might expect that it would bind to microtubules in a dimeric form that could be related to the observed x-ray structure. The image reconstruction results show that this is not the case. Nevertheless it is worthwhile to ask whether and how the x-ray dimer structure might theoretically fit onto the microtubule lattice.

We can make the theoretical assumption that one of the heads in a kinesin dimer (the "tightly" bound head) would bind in the orientation compatible with the reconstructed density and ask where the second ("loosely" bound) head would come to lie if it had the same arrangement as in the x-ray structure. In the crystals, the two heads are related by a rotation of ~120 degrees around an axis close to that of the coiled-coil neck; the two neck helices have a somewhat different conformation so that we can distinguish heads A and B within a dimer, whereas the two core motor domains are nearly superimposable. If we consider head A as the firmly bound head (Fig. 5 *B*, *D*, and *F*, *blue head*, *right*), the head B (*yellow*) would have to penetrate into the microtubule surface, which is sterically impossible. Conversely, if head B were the tightly bound head (Fig. 5, *yellow head*, *left column*), the tethered head A (*blue*) would mostly stay clear of the microtubule surface, this would therefore be the only theoretically allowed choice if one wanted to preserve the x-ray structure of the dimer. Head A would lie above the tightly bound head B, displaced in an anticlockwise direction. However, in practice this region shows no density in the reconstructions obtained with rK379. Note that this hypothetical position of the loosely bound head is different from the observed second head of ncd bound to microtubules (Fig. 4 *D*; Sosa et al., 1997*a*), emphasizing again the different behavior of these two motors.

Discussion

Orientation and Stoichiometry of Kinesin Heads Bound to Microtubules

The initial aim of this study was to explain the structure of kinesin-decorated microtubules in terms of the x-ray structures of monomeric and dimeric kinesin (Kozielski et al., 1997*a*; Sack et al., 1997).We hoped that the arrangement of dimeric kinesin heads on the microtubule surface would shed light on the mechanism of kinesin's movement along microtubules. This expectation was partly fulfilled, but in a manner that had not been anticipated. At the same time, our results explain the curious differences between previous image reconstructions of microtubules decorated with plus or minus-end directed motors (Arnal et al., 1996; Hirose et al., 1996), but again in an unforeseen fashion.

Monomeric kinesin (rK354) binds with a stoichiometry of one motor domain per tubulin heterodimer, and in an orientation comparable to that of monomeric ncd (Sosa et al., 1997*a*). It can be visualized by the left hand down rule (see above). Since the NH_2- and COOH-terminal residues are visible in our structure, we can describe the disposition of the neck helix relative to the microtubule and the core motor domain. Viewing the microtubule from outside and in standard orientation (plus end up), the motor domain lies mostly over β-tubulin, its long axis is roughly vertical, and the neck helix (thumb) projects from the upper end towards the right. This direction would be roughly tangential to the microtubule surface (Figs. 5 *E* and 6 *B*; but note that it is conceivable that the neck helix protrudes from the head in a different angle when attached to tubulin). The gearbox residues are at the upper end ("second finger"), near the neck helix. The orientation is roughly equivalent to the standard view of Sack et al. (1997) but rotated upside down. Viewed from the top (Fig. 5 *A)* the motor domain appears to wrap around the crest of the protofilament, with loop L11 (disordered in kinesin but visible in ncd) pointing clockwise and the neck helix pointing anticlockwise. This orientation of the neck is in contrast to the radial orientation expected for a lever-type mechanism of motility, sometimes postulated in analogy to the conformational change observed with the actin-dependent motor myosin (for reviews see Rayment, 1996; Holmes, 1997; Vale and Fletterick, 1997).

The dimeric kinesin construct rK379 decorates microtubules essentially in the same way and in the same orientation as monomeric constructs. Judging from the noise level at higher radii and between the heads, there is no evidence for a second head tethered to the first (Fig. 3, *F* and *G*). Since the construct is dimeric in solution and in the crystals (Kozielski et al., 1997*b*), it follows that the two heads of the kinesin dimer have come apart upon interaction with the microtubule, for reasons discussed below. The re-

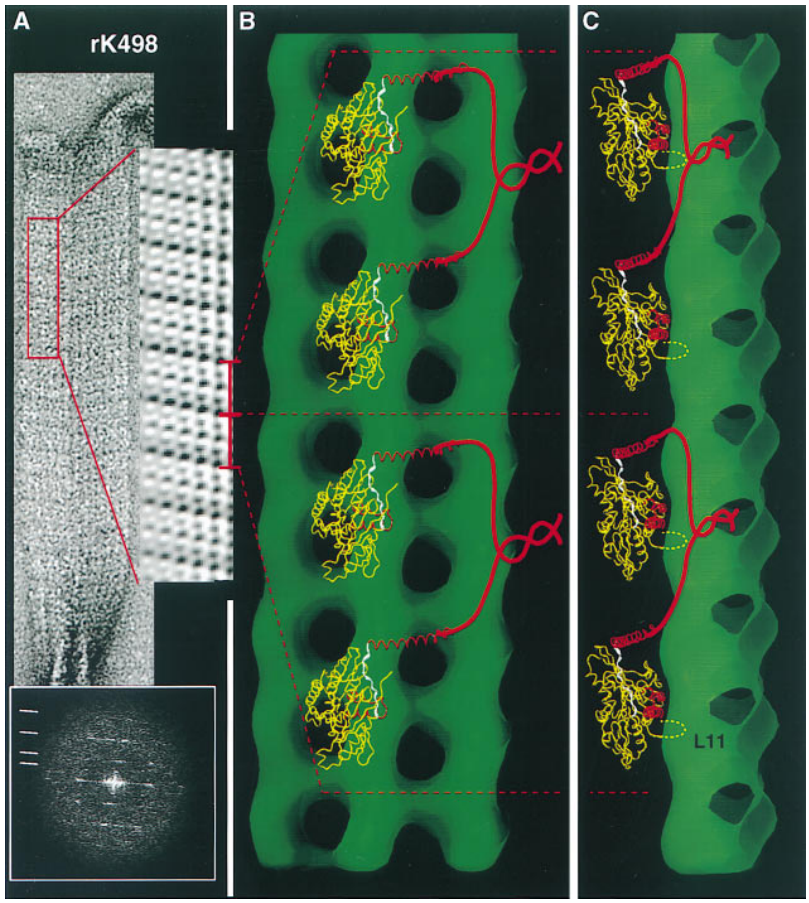

Figure 6. Model illustrating the attachment of kinesin dimers with microtubules. The three-dimensional map of microtubules is shown in surface rendering (*green*), the heads of attached kinesin dimers are shown in carbon backbone representation (*yellow*). The neck helix is red, the region beyond the neck helix is shown schematically as a red chain. Part of the region touching the microtubule surface is also shown red (α4–L12–α5). The gearbox region is highlighted in white. (*A*) Electron micrograph of two juxtaposed microtubule walls, diffraction pattern (*below*) and filtered image of boxed area (*right*), showing the periodicities of 4 nm (tubulin monomers), 8 nm (tubulin heterodimers decorated with kinesin heads), and 16 nm (pairing of kinesin dimers). *B*, front view (similar to the bound heads in Fig. 5, *E* and *F*); *C*, lateral view (similar to the bound heads in Fig. 5, *C* and *D*). The model summarizes several features described above: (*a*) the heads of dimeric kinesin decorate microtubules with a stoichiometry of one head per tubulin dimer; and (*b*) the bound heads are oriented such that the microtubule-binding loops face towards the microtubule surface and the long axis of the motor domain is vertical (similar to the bound head of ncd in Sosa et al., 1997*a*). The neck helix α7 is at the upper end (towards the microtubule plus end), the nucleotide binding pocket of the head is at the lower end (towards the microtubule minus end), and both heads of a dimer attach to microtubules in the same orientation. This arrangement is different from that of the x-ray crystal structure of the kinesin dimer; to adopt it, the coiled-coil interaction of the neck helices must be partly broken. The axial pairing of the two heads of a kinesin dimer becomes visible only with longer constructs (~400 residues or more); the paired stalk domains give rise to a 16-nm periodicity, as observed in Thormählen et al. (1998*a*), and compatible with a "tightrope" model of motility (Cross, 1995). The opened-up structure of the kinesin dimer allows the heads to move rather freely across the microtubule surface to achieve the observed step sizes (8 nm center of mass, or 16 nm per head; Svoboda et al., 1993).

sulting stoichiometry is one head per tubulin heterodimer, consistent with other biochemical and structural data (Fig. 1; Song and Mandelkow, 1993; Thormählen et al., 1998*a*), but formally in contrast to models derived from nucleotide exchange experiments (e.g., Hackney, 1994; Ma and Taylor, 1997). Since the bound kinesin head is monomeric, there is no way to fit the entire crystal structure of the dimer into the kinesin density observed by cryoelectron microscopy (Fig. 5). This structure of kinesin "dimers" is therefore clearly different from that of ncd dimers where two heads are found attached on one tubulin subunit (Fig. 4 *D*; Sosa et al., 1997*a*).

Implications for Models of Kinesin Motility

The result that the two heads of a dimeric kinesin construct bind to microtubules in a monomeric fashion has several interesting consequences. The first is that the strength of the tubulin–motor interaction partly overrides the coiled-coil interaction within the kinesin dimer, forcing the heads to come apart so that the individual kinesin molecules can bind to different tubulin heterodimers, relieving the constraints imposed by the coiled-coil necks (Thormählen et al., 1998*b*).

The separation of heads during microtubule attachment removes one of the major obstacles in modeling the motion of kinesin along microtubules: How could a kinesin dimer, consisting of two small heads only ~6-nm long and tied together directly at their base, ever achieve the observed step size of 8 nm? One theoretical possibility would be that the entire dimeric complex would "hop" 8 nm at a time, but this would mean that both heads would transiently dissociate from the microtubule simultaneously, which would be difficult to reconcile with the observed processivity (requiring at least one head to hold on to the microtubule; Berliner et al., 1995; Gilbert et al., 1995; Vale et al., 1996). Because of this constraint, most models assume that the two kinesin heads move sequentially in a "hand-over-hand" fashion, either along one protofilament ("tightrope"), or along neighboring protofilaments ("waddling;" for review see Cross, 1995). These models are consistent with important observations, such as kinetics of nucleotide exchange ("alternating head catalysis;" Hackney, 1994; Ma and Taylor, 1997; Gilbert et al., 1998), or with the movement of motors along protofilament tracks (Ray et al., 1993). However, to generate an 8-nm, center-of-mass step size, a single head would have to move 16 nm at a time. This would in turn require the heads to have long

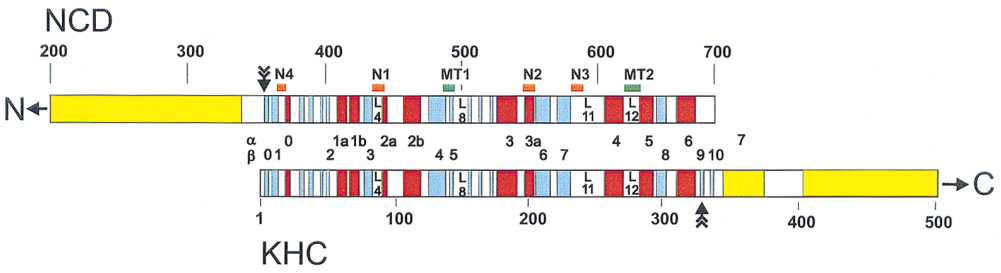

Figure 7. Diagram of coiled-coil segments coil around motor domains of ncd (*top*) and kinesin (*bottom*). Secondary structure elements in the motor domain are shown in blue (β strands) and red (α helix), the numbering of elements (between the bars) follows that of Kull et al. (1996) and Sablin et al. (1996) (differences between the structures are omitted here for simplicity). Coiled-coil sequences are shown in yellow (predicted, following Lupas et al., 1991) or observed (for the neck of kinesin). Note that ncd has an extended sequence of predicted coiled-coil preceding the motor domain (residues ~190–340), whereas kinesin has only a short coiled-coil following the motor domain (residues Ala339–Trp370, predicted and experimentally observed), followed by a disordered loop (residues 370–406) before the subsequent stalk-I coiled-coil. The conserved gearbox regions are indicated by arrows (Case et al., 1997). Residue numbers are given above (*NCD*) or below (*KHC*).

and semi-independent necks. Accordingly, the models for kinesin movement are usually shown with long and free necks, but this is clearly in contradiction to the observed crystal structure of kinesin dimers (Kozielski et al., 1997*a*). The resolution of this dilemma is to separate the heads specifically upon interaction with microtubules, as observed in this study.

The gain in freedom for the heads can be estimated as follows. The length of the neck helix (Ala339–Trp370) is ~4.6 nm (0.15 nm per helical residue). This is followed by a disordered region which extends to another predicted coiled-coil starting around residue Val406. Assuming an average chain length of 0.2–0.3 nm per residue, this would amount to ~10–15 nm, giving a total of ~15–20 nm per head. This would generate a "long leash," allowing the two heads to be separated by twice this value (~30–40 nm) more than sufficient to cover the distance of 16 nm per head. In addition, we note that the strands β9 and β10 connecting the motor domain to the neck helix and harboring the gearbox residues (Fig. 6, *white*) are only weakly attached to the core motor and could possibly detach during some stage of the movement, giving even more freedom of movement (Romberg et al., 1998).

Even if the two heads of a kinesin dimer are separated on the microtubule surface one would expect that longer constructs, or whole kinesin dimers, would stay in contact further downstream, for example from the second coiled-coil region onwards (e.g., starting around residue 406). In principle, it should therefore be possible to detect a pairing of kinesin stalk domains on the microtubule surface in the case of longer constructs. For full-length kinesin, this is technically difficult to show experimentally because the long stalks prevent periodic binding of kinesin to microtubules (a prerequisite for image analysis). However, intermediate constructs (up to 500 residues in length) tend to reveal an additional 16 nm layer line, twice the repeat of a tubulin heterodimer (Thormählen et al., 1998*a*; and Fig. 6 *A*). This is interpreted as a pairing of kinesin monomers into dimers in the axial direction, arguing for a tightrope model where the two monomers of a dimer bind to successive tubulin subunits along one protofilament, as illustrated in the models of Fig. 6 (*B*, *front view*, and *C*, *lateral view of left edge*). The 16-nm periodicity would arise from the stalk domain common to both monomers of a dimer.

Comparison between Kinesin and ncd

Why do double-headed kinesin and ncd constructs look and move differently on a microtubule, in spite of their similar motor domain? This question has been addressed in several recent studies based on image reconstruction and biochemical data. There appears to be a consensus that monomeric kinesin and ncd occupy the same binding site on microtubules, both from binding studies experiments (Lockhart et al., 1995; Song and Endow, 1996) and image reconstruction (Hoenger and Milligan, 1997). The firmly bound head of ncd was compared with its x-ray structure (Sablin et al., 1996), resulting in the orientation proposed by Sosa et al. (1997*a*). In the present work we find a very similar orientation (left hand down when microtubule is plus end up) by comparing the image reconstruction of rat kinesin with its x-ray structure (Sack et al., 1997).

Differences on the level of observation and interpretation exist when one compares double-headed kinesin and ncd. The dimeric construct ncd-Δ295-700 clearly attaches to microtubules as a dimer, one head firmly bound, the second tethered to the first, as in Fig. 4 *D* (Arnal et al., 1996; Hirose et al., 1996; Sosa et al., 1997*a*). Both heads had roughly the volume expected for their molecular weight. In the case of "dimeric" kinesin the "second head" had only ~20% of its expected mass, which was interpreted in terms of disorder (Arnal et al., 1996; Hirose et al., 1996; Amos and Hirose, 1997). On the basis of our results we would question that interpretation; the additional density could simply be accounted for by the additional mass of the dimeric construct, compared with the monomeric construct (401–340 = 61 residues or 18%). Thus, the reconstructions of Arnal et al. (1996) and Hirose et al. (1996) would be compatible with our interpretation of only one head bound per tubulin dimer. In our case the difference amounts to only 379–354 = 25 residues or 7%, which is not enough to make a visible contribution at the limited resolution. Alternatively, partial decoration by the second head may be more likely with the slightly longer constructs used by Arnal et al. (1996) and Hirose et al. (1996). This partial decoration may reveal a reduced mass as found in their reconstructions. Nevertheless this would still support our hypothesis of a (preferred) disassembly of the dimer neck region once one of the motor binds to tubulin.

The differences in interpretation had consequences for proposed mechanisms of motility. The second head of ncd and the (interpreted) second head of kinesin had different orientations on the microtubule lattice, and it was thought that this was related to their different directionality. Our results argue that this view should be abandoned. The determination of directionality appears to be more subtle than apparent from gross head–head interactions, involving short gearbox sequences that may mediate between the core motor domain and the neck helix (Case et al., 1997; Henningsen and Schliwa, 1997; Romberg et al., 1998). Moreover, it is likely that the directionality is built into individual motor molecules since there are monomeric kinesins (e.g., KIF1A, KIF1B; Nangaku et al., 1994; Okada et al., 1995), and since even single chains of dimeric motors can generate movement (Berliner et al., 1995, Inoue et al., 1997).

The question that remains to be explained is Why do dimeric ncd constructs remain joined upon attaching to microtubules, while kinesin constructs come apart? The answer is likely to be the strength of the intra-dimer interaction, coupled possibly with conformational differences. The intra-dimer interaction is thought to rest mainly on the coiled-coil interaction in the neck and stalk region (although this might be modulated by interactions with the motor domain and with tubulin). Since the NH_2 and COOH termini of the motor domain are spatially very close to one another the transition to the neck helix would also be expected to be similar (thus far the structure of the transition region is only known for kinesin; see Sack et al., 1997). Fig. 7 illustrates the predicted coiled-coil probability (using the COILS algorithm; Lupas et al., 1991); the kinesin neck is COOH-terminal to the motor domain, the ncd neck is NH_2-terminal. The strength of the coiled-coil interaction appears to be weaker in the initial neck (nearest the motor) than in segments further away (Morii et al., 1997; Tripet et al., 1997). This argues in favor of a mechanism whereby the two heads of a dimer separate during some step in the motile cycle, even in the case of ncd. The coiled-coil predictions alone do not clearly distinguish between ncd's tendency to stay dimeric on a tubulin subunit, whereas kinesin heads are forced apart and settle on different tubulin subunits. However, the predictions provide a testable hypothesis that can be addressed experimentally using mutant forms of kinesin or ncd.

A final point concerns the possibility of a lever arm mechanism of motility. This mechanism is currently discussed for the case of the actin-dependent motor myosin since, in this case, speed of movement depends on the length of the neck helix (Anson et al., 1996; Uyeda et al., 1996), since the neck helix undergoes nucleotide-dependent angular motions (Whittaker et al., 1995*b*), and since the x-ray structure of myosin shows related changes in the nucleotide-binding domain (Fisher et al., 1995; Smith and Rayment, 1996). The lever arm hypothesis presumes that the neck points away from the actin filament, towards the myosin filament, and generates movement by swinging (for reviews see Rayment, 1996; Holmes, 1997). In the case of kinesin (and probably ncd), the neck helix does not point away from the microtubule surface, but rather tangentially to it (Fig. 6), and—unlike with myosin—the coiled-coil becomes separated upon binding to microtubules. It is therefore not likely that myosin-type models can be applied to microtubule motors. Further structural studies with variants of motor proteins should reveal whether an angular change in the neck or stalk region is involved in the movement.

We are grateful to P. Tittmann (ETH, Zurich, Switzerland) for help with specimen preparation; M. Whittaker (The Scripps Institute, La Jolla, CA) for help with the transfer of programs to Zürich; S. Brady (University of Texas, Dallas, TX) for providing the original clone of rat kinesin; R. Milligan (The Scripps Institute) and E. Mandelkow (Hamburg) for many discussions on structural and biochemical aspects.

S. Sack is a recipient of a fellowship from the Friedrich-Ebert Foundation. The project was supported by the Deutsche Forschungsgemeinschaft and the Swiss Science Foundation.

Received for publication 8 October 1997 and in revised form 2 February 1998.

References

Amos, L.A., and K. Hirose. 1997. The structure of microtubule-motor complexes. *Curr. Opin. Cell Biol.* 9:4–11.

Anson, M., M.A. Geeves, S.E. Kurzawa, and D.J. Manstein. 1996. Myosin motors with artificial lever arms. *EMBO (Eur. Mol. Biol. Organ.) J.* 15:6069–6074.

Arnal, I., F. Metoz, S. DeBonis, and R.H. Wade. 1996. Three-dimensional structure of functional motor proteins on microtubules. *Curr. Biol.* 6:1265–1270.

Berliner, E., E.C. Young, K. Anderson, H.K. Mahtani, and J. Gelles. 1995. Failure of a single-headed kinesin to track parallel to microtubule protofilaments. *Nature.* 373:718–721.

Brady, S.T. 1995. A kinesin medley: biochemical and functional heterogeneity. *Trends Cell Biol.* 5:159–164.

Case, R.B., D.W. Pierce, N. Hom-Booher, C.L. Hart, and R.D. Vale. 1997. The directional preference of kinesin motors is specified by an element outside of the motor catalytic domain. *Cell.* 90:959–966.

Cole, D., and J.M. Scholey. 1995. Structural variations among the kinesins. *Trends Cell Biol.* 5:259–262.

Coppin, C.M., J.T. Finer, J.A. Spudich, and R.D. Vale. 1996. Detection of sub-8-nm movements of kinesin by high-resolution optical-trap microscopy. *Proc. Natl. Acad. Sci. USA.* 93:1913–1917.

Correia, J.J., S.P. Gilbert, M.L. Moyer, and K.A. Johnson. 1995. Sedimentation studies on the kinesin motor domain constructs K401, K366, and K341. *Biochemistry.* 34:4898–4907.

Crevel, I.M., A. Lockhart, and R.A. Cross. 1996. Weak and strong states of kinesin and ncd. *J. Mol. Biol.* 257:66–76.

Cross, R.A. 1995. On the hand-over-hand footsteps of kinesin heads. *J. Muscle Res. Cell Motil.* 16:91–94.

Dubochet, J., M. Adrian, J. Lepault, and A.W. McDowall. 1985. Cryo-electron microscopy of vitrified biological specimens. *Trends Biochem. Sci.* 10:143–146.

Fisher, A.J., C.A. Smith, J.B. Thoden, R. Smith, K. Sutoh, H.M. Holden, and I. Rayment. 1995. X-ray structures of the myosin motor domain of *Dictyostelium discoideum* complexed with MgADP.BeFx and MgADP.AlF4. *Biochemistry.* 34:8960–8972.

Gilbert, S.P., M.R. Webb, M. Brune, and K.A. Johnson. 1995. Pathway of processive ATP hydrolysis by kinesin. *Nature.* 373:671–676.

Gilbert, S.P., M.L. Moyer, and K.A. Johnson. 1998. Alternating site mechanism of the kinesin ATPase. *Biochemistry.* 37:792–799.

Goldstein, L.S.B. 1993. With apologies to Scheherazade: Tails of 1001 kinesin motors. *Annu. Rev. Genet.* 27:319–351.

Gross, H., K. Krusche, and P. Tittmann. 1990. Recent progress in high resolution shadowing for biological TEM. *XIIth Intl. Cong. Electron Microsc.* Seattle, WA. 510–511.

Hackney, D.D. 1994. Evidence for alternating head catalysis by kinesin during microtubule-stimulated ATP hydrolysis. *Proc. Natl. Acad. Sci. USA.* 91: 6865–6869.

Harrison, B.C., S.P. Marchese-Ragona, S.P. Gilbert, N. Cheng, A.C. Steven, and K.A. Johnson. 1993. Decoration of the microtubule surface by one kinesin head per tubulin heterodimer. *Nature.* 362:73–75.

Henningsen, U., and M. Schliwa. 1997. Reversal of the direction of movement of a molecular motor. *Nature.* 389:93–96.

Hessler, D., S.J., Young, and M.H. Ellisman. 1996. A flexible environment for the visualization of three-dimensional biological structures. *J. Struct. Biol.* 116:113–119.

Hirose, K., A. Lockhart, R.A. Cross, and L.A. Amos. 1995. Nucleotide dependent angular change in kinesin motor domain bound to tubulin. *Nature.* 376: 277–279.

Hirose, K., A. Lockhart, R.A. Cross, and L.A. Amos. 1996. Three-dimensional cryoelectron microscopy of dimeric kinesin and ncd motor domains on mi-

crotubules. *Proc. Natl. Acad. Sci. USA.* 93:9539–9544.
Hoenger, A., and R.A. Milligan. 1996. Polarity of 2-D and 3-D maps of tubulin sheets and motor decorated sheets. *J. Mol. Biol.* 263:114–119.
Hoenger, A., and R.A. Milligan. 1997. Motor domains of kinesin and ncd interact with microtubule protofilaments with the same binding geometry. *J. Mol. Biol.* 265:553–564.
Hoenger, A., E.P. Sablin, R.D. Vale, R.J. Fletterick, and R.A. Milligan. 1995. Three-dimensional structure of a tubulin-motor-protein complex. *Nature.* 376:271–274.
Holmes, K.C. 1997. The swinging lever-arm hypothesis of muscle contraction. *Curr. Biol.* 7:112–118.
Howard, J. 1996. The movement of kinesin along microtubules. *Annu. Rev. Physiol.* 58:703–729.
Hua, W., E.C. Young, M.L. Fleming, and J. Gelles. 1997. Coupling of kinesin steps to ATP hydrolysis. *Nature.* 388:390–393.
Huang, T.G., J. Suhan, and D.D. Hackney. 1994. Drosophila kinesin motor domain extending to amino acid position 392 is dimeric when expressed in *Escherichia coli*. *J. Biol. Chem.* 269:16502–16507.
Inoue, Y., Y.Y. Toyoshima, A.H. Iwane, S. Morimoto, H. Higuchi, and T. Yanagida. 1997. Movements of truncated kinesin fragments with a short or an artificial flexible neck. *Proc. Natl. Acad. Sci. USA.* 94:7275–7280.
Jiang, W., M.F. Stock, X. Li, and D.D. Hackney. 1997. Influence of the kinesin neck domain on dimerization and ATPase kinetics. *J. Biol. Chem.* 272:7626–7632.
Jones, T.A., J.Y. Zou, S.W. Cowan, and M. Kjeldgaard. 1991. Improved methods for building protein models in electron density maps and the location of errors in these models. *Acta Crystallogr. A.* 47:110–119.
Kikkawa, M., T. Ishikawa, T. Wakabayashi, and N. Hirokawa. 1995. Three-dimensional structure of the kinesin head-microtubule complex. *Nature.* 376: 274–277.
Kozielski, F., S. Sack, A. Marx, M. Thormählen, E. Schönbrunn, V. Biou, A. Thompson, E.-M. Mandelkow, and E. Mandelkow. 1997*a*. The crystal structure of dimeric kinesin and implications for microtubule-dependent motility. *Cell.* 91:985–994.
Kozielski, F., E. Schönbrunn, S. Sack, J. Müller, S.T. Brady, and E. Mandelkow. 1997*b*. Crystallization and preliminary X-ray analysis of the single-headed and double-headed motor protein kinesin. *J. Struct. Biol.* 119:28–34.
Kull, F.J., E. Sablin, P. Lau, R. Fletterick, and R. Vale. 1996. Crystal structure of the kinesin motor domain reveals a structural similarity to myosin. *Nature.* 380:550–554.
Lockhart, A., I.M. Crevel, and R.A. Cross. 1995. Kinesin and ncd bind through a single head to microtubules and compete for a shared MT binding site. *J. Mol. Biol.* 249:763–771.
Lupas, A., M. Van Dyke, and J. Stock. 1991. Predicting coiled coils from protein sequences. *Science.* 252:1162–1164.
Ma, Y.Z., and E.W. Taylor. 1997. Interacting head mechanism of microtubule-kinesin ATPase. *J. Biol. Chem.* 272:724–30.
Mandelkow, E.-M., and E. Mandelkow. 1985. Unstained microtubules studied by cryo-electron microscopy: substructure, supertwist and disassembly. *J. Mol. Biol.* 181:123–135.
Mandelkow, E.-M., M. Herrmann, and U. Rühl. 1985. Tubulin domains probed by limited proteolysis and subunit-specific antibodies. *J. Mol. Biol.* 185:311–327.
Mandelkow, E.-M., R. Schultheiss, R. Rapp, M. Müller, and E. Mandelkow, 1986. On the surface lattice of microtubules: Helix starts, protofilament number, seam and handedness. *J. Cell Biol.* 102:1067–1073.
Marx, A., M. Thormählen, S. Sack, and E. Mandelkow. 1998. Crystal structure of kinesin and interaction with microtubules. *Eur. Biophysics J.* In press.
Morii, H., T. Takenawa, F. Arisaka, and T. Shimizu. 1997. Identification of kinesin neck region as a stable alpha-helical coiled coil and its thermodynamic characterization. *Biochemistry.* 36:1933–1942.
Nangaku, M., R. Sato-Yoshitake, Y. Okada, Y. Noda, R. Takemura, H.Yamazaki, and N. Hirokawa. 1994. KIF1B, a novel microtubule plus end-directed monomeric motor protein for transport of mitochondria. *Cell.* 79:1209–1220.
Okada, Y., H. Yamazaki, Y. Sekine-Aizawa, and N. Hirokawa. 1995. The neuron-specific kinesin superfamily protein KIF1A is a unique monomeric motor for anterograde axonal transport of synaptic vesicle precursors. *Cell.* 81: 769–780.
Ray, S., E. Meyhofer, R.A. Milligan, and J. Howard. 1993. Kinesin follows the microtubule's protofilament axis. *J. Cell Biol.* 121:1083–1093.
Rayment, I. 1996. Kinesin and myosin: molecular motors with similar engines. *Structure.* 4:501–504.
Romberg, L., D.W. Pierce, and R.D. Vale. 1998. Role of the kinesin neck region in processive microtubule-based motility. *J. Cell Biol.* 140:1407–1416.
Sablin, E.P., F.J. Kull, R. Cooke, R.D. Vale, and R.J. Fletterick. 1996. Crystal structure of the motor domain of the kinesin-related motor ncd. *Nature.* 380: 555–559.
Sack, S., J. Müller, A. Marx, M. Thormählen, E.-M. Mandelkow, S.T. Brady, and E. Mandelkow. 1997. X-ray structure of motor and neck domains from rat brain kinesin. *Biochemistry.* 36:16155–16165.
Schnitzer, M.J., and S.M. Block. 1997. Kinesin hydrolyses one ATP per 8-nm step. *Nature.* 388:386–90.
Schroeter, J., and J.-P. Bretaudiere. 1996. SUPRIM: easily modified image processing software. *J. Struct. Biol.* 116:131–137.
Smith, C.A., and I. Rayment. 1996. X-ray structure of the magnesium(II).ADP.vanadate complex of the *Dictyostelium discoideum* myosin motor domain to 1.9 Å resolution. *Biochemistry.* 35:5404–5417.
Song, H., and S.A. Endow. 1996. Binding sites on microtubules of kinesin motors of the same or opposite polarity. *Biochemistry.* 35:11203–11209.
Song, Y.H., and E. Mandelkow. 1993. Recombinant kinesin motor domain binds to β-tubulin and decorates microtubules with a B surface lattice. *Proc. Natl. Acad. Sci. USA.* 90:1671–1675.
Sosa, H., and R.A. Milligan. 1996. Three-dimensional structure of ncd-decorated microtubules obtained by a back-projection method. *J. Mol. Biol.* 260: 743–755.
Sosa, H., D.P. Dias, A. Hoenger, M. Whittaker, E. Wilson-Kubalek, E. Sablin, R.J. Fletterick, R.D. Vale, and R.A. Milligan. 1997*a*. A model for the microtubule-Ncd motor protein complex obtained by cryo-electron microscopy and image analysis. *Cell.* 90:217–224.
Sosa, H., A. Hoenger, and R.A. Milligan. 1997*b*. Three different approaches for calculating the 3-dimensional structure of microtubules decorated with kinesin motor domains. *J. Struct. Biol.* 118:149–158.
Svoboda, K., C.F. Schmidt, B.J. Schnapp, and S.M. Block. 1993. Direct observation of kinesin stepping by optical trapping interferometry. *Nature.* 365:721–727.
Thormählen, M., A. Marx, S.A. Müller, Y.-H. Song, E.-M. Mandelkow, U. Aebi, and E. Mandelkow. 1998*a*. Interaction of monomeric and dimeric kinesin with microtubules. *J. Mol. Biol.* 275:795–809.
Thormählen, M., A. Marx, S. Sack, and E. Mandelkow. 1998*b*. The coiled-coil helix in the neck of kinesin. *J. Struct. Biol.* In press.
Tripet, B., R.D. Vale, and R.S. Hodges. 1997. Demonstration of coiled-coil interactions within the kinesin neck region using synthetic peptides—implications for motor activity. *J. Biol. Chem.* 272:8946–8956.
Tucker, C., and L.S.B. Goldstein. 1997. Probing the kinesin–microtubule interaction. *J. Biol. Chem.* 272:9481–9488.
Uyeda, T.Q., P.D. Abramson, and J.A. Spudich. 1996. The neck region of the myosin motor domain acts as a lever arm to generate movement. *Proc. Natl. Acad. Sci. USA.* 93:4459–4464.
Vale, R.D., and R.J. Fletterick. 1997. The design plan of kinesin motors. Annu. Rev. Cell Dev. Biol. 13:745–777.
Vale, R.D., T. Funatsu, D.W. Pierce, L. Romberg, Y. Harada, and T. Yanagida. 1996. Direct observation of single kinesin molecules moving along microtubules. *Nature.* 380:451–453.
Wade, R.H., D. Chrètien, and D. Job. 1990. Characterization of microtubule protofilament numbers; how does the surface lattice accommodate? *J. Mol. Biol.* 212:775–786.
Wade, R.H., R. Horowitz, and R.A. Milligan. 1995. Toward understanding the structure and interactions of microtubules and motor proteins. PROTEINS: structure, function, and genetics 23:502–509.
Walker, R.A. 1995. Ncd and kinesin motor domains interact with both alpha- and beta-tubulin. *Proc. Natl. Acad. Sci. USA.* 92:5960–5964.
Whittaker, M., B.O. Carragher, and R.A. Milligan. 1995*a*. PHOELIX: a package for semi-automated helical reconstruction. *Ultramicroscopy.* 58:245–259.
Whittaker, M., E.M. Wilson-Kubalek, J.E. Smith, L. Faust, R.A. Milligan, and H.L. Sweeney. 1995*b*. A 35Å movement of smooth muscle myosin on ADP release. *Nature.* 378:748–751.
Woehlke, G., A.K. Ruby, C.L. Hart, B. Ly, N. Hom-Booher, and R.D. Vale. 1997. Microtubule interaction site of the kinesin motor. *Cell.* 90:207–216.